Seismic stratigraphy of the northern area of Punta Bandera (Lago Argentino, southern Patagonia)

Jorge G. Lozano [a,b,*], Florencia B. Restelli [a,b], Stefania Bunicontro [a,b], Salomé C. Salvó Bernárdez [a,b], Donaldo M. Bran [a,b], Maurizio Grossi [c], Emanuele Lodolo [c], Alejandro A. Tassone [a,b]

[a] *Universidad de Buenos Aires, Facultad de Ciencias Exactas y Naturales, Depto. De Ciencias Geológicas, Buenos Aires, Argentina*
[b] *CONICET-Universidad de Buenos Aires, Instituto de Geociencias Básicas, Aplicadas y Ambientales de Buenos Aires (IGeBA), Buenos Aires, Argentina*
[c] *Istituto Nazionale di Oceanografia e di Geofisica Sperimentale (OGS), Trieste, Italy*

A B S T R A C T

Lago Argentino is one of the largest lakes in Patagonia. Some of its arms host calving glaciers that flow from the southern Patagonian Ice Field. The best known of these is the Perito Moreno glacier. Although recent studies have reconstructed part of glacier dynamics in the southern arms of Lago Argentino, there are no studies yet for the northern arms. A high-resolution seismic survey was carried out in the northern area of Punta Bandera, i.e., in the sector between the Brazo Norte and the Canal de los Témpanos to characterize the stratigraphy of the sedimentary fill of the lake and identify the main unconformities related to glacial dynamics. Eight seismic facies grouped into two seismic units were mapped, and ten unconformities were recognized. Based on the acquired data, a bathymetric grid was created for the first time to obtain a morphological representation of the lake floor and access to a previously unmapped area of Lago Argentino. The analysis of the geometries and acoustic properties of the different seismic facies identified, correlated with the available information on land moraines, has allowed us to partially reconstruct the advance and retreat phases of the glacial lobes that formerly were present in the two arms of the lake, although the temporal assignments are still speculative due to the lack of calibrations with boreholes. Nevertheless, this study provides important information for deciphering the glaciation history of a key sector of the southern Patagonian Ice Field during the late Pleistocene/Holocene. The data show that the northern and southern areas have different lake floor morphologies, with the southern, shallower area of the Canal de los Témpanos being glaciated first than the northern, more overdeepened area of the Brazo Norte.

1. Introduction

Lago Argentino, located in Santa Cruz Province, Argentina (Fig. 1; Table 1), consists of a large elliptical body of water nearly 60 km long and 15 km wide with several lake arms that develop in a series of W-E and N–S trending glacial valleys.

The lake is part of the "Parque Nacional Los Glaciares", a natural park characterized by some of the most important glaciers of the Southern Patagonian Ice Field (SPI). The most famous of there is the Perito Moreno Glacier, which has been declared an UNESCO World Heritage Site. In contrast to most glaciers in this area, which have retreated significantly over the last 50 years (Davies et al., 2020), the Perito Moreno Glacier has a relatively stable mass balance with minimal fluctuations in the ice front (Malagnino and Strelin, 1990; Skvarca et al., 2002; Skvarca and Naruse, 2006; Sakakibara and Sugiyama, 2014; Minowa et al., 2017).

Lago Argentino consists of an ellipsoidal main body of water running in an E-W direction with some structurally controlled, deeply incised glacial valleys (Lodolo et al., 2020a). During ice retreat, a large proglacial lake formed along the eastern ice margin, which was dammed between the ice sheet and higher ground moraines (Davies et al., 2020).

Due to its particular location within the lake, the Punta Bandera area is an important sector for the study of sedimentation processes and the control of the subaqueous morphology of the Lago Argentino basin. It is located at the confluence of Brazo Norte and Canal de los Témpanos (Fig. 2) and represents an area where the dynamics of two glacial lobes

---

* Corresponding author. Universidad de Buenos Aires, Facultad de Ciencias Exactas y Naturales, Depto. De Ciencias Geológicas. Buenos Aires, Argentina.
 *E-mail address:* lozano@gl.fcen.uba.ar (J.G. Lozano).

interacted before the last 12 kyr.

Previous studies focused on seismic stratigraphy, morphology analysis, and structural controls acting in the formation of lacustrine basins with an influence of recent glacial dynamics (Lodolo et al., 2002, 2003, 2007, 2012; Lippai et al., 2004; Waldmann et al. 2008, 2009, 2010a, 2010b, b; Esteban et al., 2014; Lozano et al. 2018a, 2018b). In particular, some geophysical studies have been carried out in the southern arms of Lago Argentino, where an initial characterization of the above questions has been made (Lodolo et al. 2020a, 2020b; Lozano et al., 2020c, 2021b, 2022). The Holocene glacial history of the Lago Argentino basin is well documented on land, especially during the last 12 kyr (peat cores with ^{14}C dating and boulders for samples for cosmogenic ^{10}Be measurement; Strelin et al., 2014). Subaqueous evidence for the

Table 1
Physical dimensions and characteristics of Lago Argentino. The data source is the Subsecretaría de Recursos Hídricos (Quirós et al., 1988; Calcagno et al., 1995).

	Lago Argentino
Elevation of the lake level	187 m.a.s.l.
Maximum depth of the lake	500 m
Average depth of the lake	150 m
Lake area	1466 km2
Catchment area	17,000 km2
Effluent rivers	Rio Santa Cruz
Drainage	Atlantic Ocean
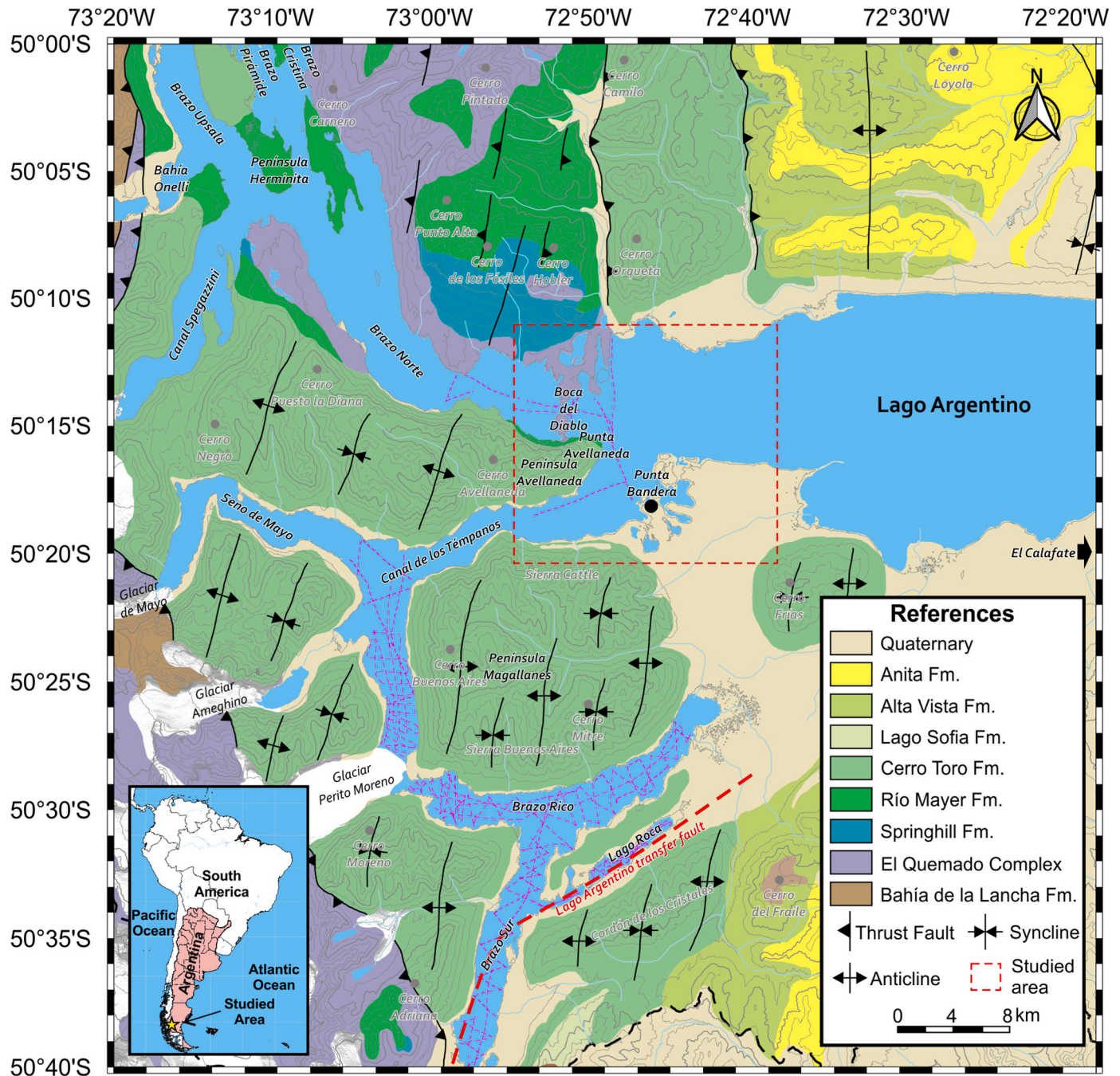
Fig. 1. Geology of the Lago Argentino area. The red dashed box shows the studied area, which is shown in Fig. 2. The geology and structure of the area are based on Nullo et al. (2006) and Ghiglione et al. (2009).

Brazo Rico and Brazo Sur has been correlated with these studies (Lodolo et al. 2020a, 2020b; Lozano et al., 2021b), providing a more complete model for the southern area. However, as the extent of the northern arms of Lago Argentino is larger, information on the complete coverage of the lake basin is still lacking. In this context, the high-resolution seismic data acquired in the northern area of Punta Bandera provide an important opportunity to complete the regional overview of the ice extent in the flooded lake basin. The seismic dataset was analyzed with the goal of defining the seismic stratigraphy and unconformities and creating a bathymetric grid for the northern area of Punta Bandera. The main objective of this research is to analyze and reconstruct the sedimentary history of the Canal de los Témpanos and the Brazo Norte confluence zone in relation to the glacial fluctuations in the region during the Late Pleistocene/Holocene.

The results of this work will be useful to complete the models already

under development on glacial advances during the late Pleistocene/ Holocene in Lago Argentino and then to decipher the implications of the glaciation history of the SPI. The stratigraphy of the lake's sedimentary fill could lead to a complete reconstruction of glacial retreat during the last 12.3 cal kyr, a time when the Punta Bandera area was ice-free (peat bog developed, dated for ^{14}C; Strelin et al., 2011).

2. Regional framework

2.1. Geomorphology

The area around Lago Argentino (Fig. 1) is characterized by several tectonic and exogenous processes that have shaped the present-day landscape of this Patagonian lake. The deformation processes resulted in a structure characterized by a fold and overthrust belt with N- and
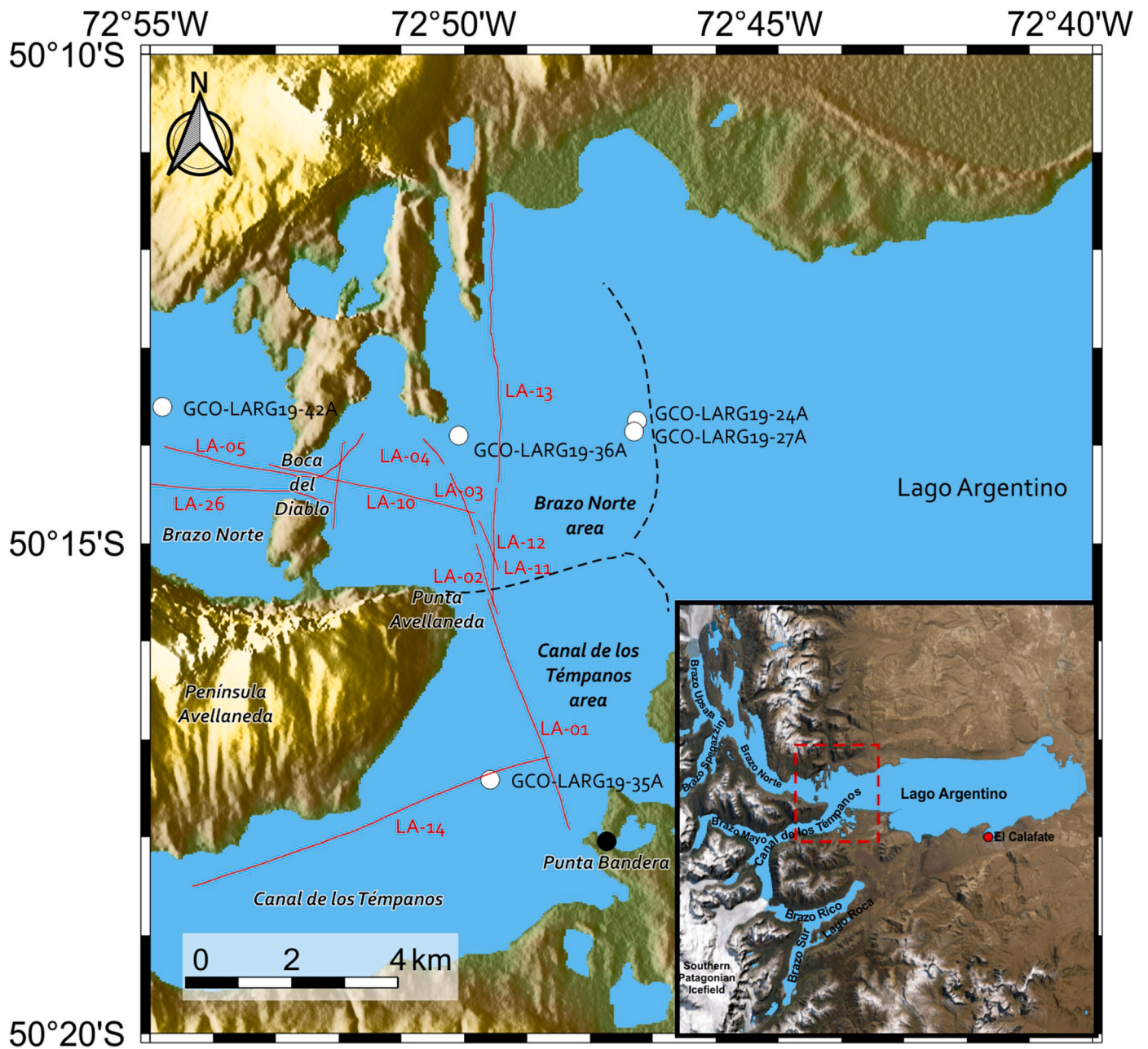

Fig. 2. Location map of the central area of Lago Argentino, near the confluence of the Brazo Norte with the Canal de los Témpanos. The most important geographical reference points are shown. The insets show the location of the study area. The white dots show the location of gravity cores in the lake, taken from Van Wyk de Vries et al. (2022)

NW-oriented anticlines, overthrusts and backthrusts with N–S strikes (Kraemer et al., 2002; Ghiglione et al., 2009) and some overthrust structures with E-W strikes along the axis of Lago Argentino and Lago Viedma (Ghiglione et al., 2009). The present landscape is essentially a mountain range with large elevations and deep alpine glacial valleys, with the eastern part dominated by highland relief on the north and south sides of Lago Argentino.

Glacial erosion is closely linked to spatial patterns of ice flow and sediment transport and deposition (Alley et al., 1997). Overdeepenings in glacial valleys can form because positive ice surface gradients allow ice and subglacial water to ascend unfavorable subglacial slopes. The removal of sediments by ice and water flows thus allows continued erosion of the ice bed, further enlarging the deepening basin (Cook and Swift, 2012; Patton et al., 2016).

A series of large proglacial lakes formed at the eastern ice margin of the SPI following the retreat of ice after the Last Glacial Maximum (LGM; Caldenius, 1932; Mercer, 1969, 1976; McCulloch et al., 2000; Glasser et al., 2008; Glasser and Jansson, 2008; Coronato and Rabassa, 2011). However, there is significant controversy concerning the occurrence and timing of late-glacial and subsequent advances. Coronato and Rabassa (2011) showed an LGM that roughly matched the global LGM, whereas Davies et al. (2020) determined a local LGM of about 35 ka. Nevertheless, the resulting lakes were dammed between the ice sheet and the moraine deposits on the western and eastern margins (Caldenius, 1932; McCulloch and Bentley, 1998; Glasser et al., 2016; Thorndycraft et al., 2019).

The SPI is the largest ice mass in Patagonia with a size of 13,219 km^2 and an average elevation of 3400 m (Davies and Glasser, 2012). The ice thickness reaches 1.5 km, and base elevation is below sea level (Gourlet et al., 2016). The eastern boundary of the SPI provides evidence of past glaciations, characterized by four chronostratigraphically confirmed main ice lobes. In the studied area, the Lago Argentino lobe is one of them (Strelin et al., 2011, 2014; Kaplan et al., 2016). This lobe is bounded by several moraine sequences studied by Strelin and Malagnino (2000) and Strelin et al. (2011) through the recognition and age dating of the Puerto Bandera moraines. Pre-LGM glaciations were delineated eastward along the Rio Santa Cruz valley (Strelin and Malagnino, 1996).

The Punta Bandera area is located at the confluence of the Brazo Norte and Canal de los Témpanos and east of the main part of Lago Argentino. The nearest outlet glaciers flowing into Lago Argentino are the Ameghino, Mayo, and Perito Moreno glaciers from the Canal de los Témpanos and the Spegazzini glacier from the Brazo Norte (Fig. 2). Of these glaciers, Perito Moreno is in a stable equilibrium with the climate and is subject to periodic fluctuations due to the unique geometry of the calving front and the morphology of the lake floor (Stuefer et al., 2007; Davies and Glasser, 2012), while the other glaciers of the SPI have been retreating since the Little Ice Age (Davies and Glasser, 2012). Between 2000 and 2016, the SPI suffered a mass loss rate of -11.84 ± 3.3 Gt/yr (Malz et al., 2018).

A compilation of Holocene glacier advances in the southernmost Andes is presented by Kilian and Lamy (2012). The oscillations of the SPI were primarily controlled by paleotemperatures and the intensity and latitudinal position of the southwest wind belt (SWW) 12 kyr ago. Most of the influences that occurred after 5.5 kyr BP were likely caused primarily by a short-term increase in SWW strength and associated increased precipitation/accumulation (Kilian and Lamy, 2012).

2.2. Seismic stratigraphy of the southern arms of Lago Argentino

Previous studies have been carried out in the southern arms of Lago Argentino-Brazo Rico and Brazo Sur (e.g., Lodolo et al., 2020a, b; Lozano et al., 2020c, 2021b, 2022), and focused on characterizing the seismic stratigraphy and morphostructure of the area.

The Brazo Rico, an east-west trending elongated body of southern Lago Argentino, overlaps in its central part with the north-south trending arm of the lake, the Brazo Sur. The Frias Glacier bounded the southern margin of Brazo Sur until the last 6.5 kyr, while the ice front of the Perito Moreno Glacier shaped the western margin of Brazo Rico from 12.6 kyr to present-day (for ^{14}C dated peat cores and samples for cosmogenic ^{10}Be measurements; Strelin et al., 2011, 2014; Kaplan et al., 2016; Lozano et al., 2021b).

The seismic records in these southern lake arms show the presence of two main units: (i) a lower unit of glacial origin and (ii) an upper unit of glaciolacustrine origin. The lower unit is characterized by a rough morphology and seismic facies containing discontinuous reflections often characterized by diffractions and transparent intervals. The upper glaciolacustrine unit consists of a broad distribution of continuous and high-amplitude, horizontal to divergent reflections. The glaciolacustrine unit has the thickest packages in the morphologic depressions of the lake bedrock.

3. Methodology

3.1. Seismic acquisition

In December 2009, a total of about 46 km of high-resolution single-channel seismic lines were acquired in the northern area of Punta Bandera at the confluence of the Brazo Norte with the Canal de Los Témpanos (Fig. 3). This seismic data was acquired using a single-channel, 10-m oil-filled streamer and a Boomer seismic source that allows a 300-J pulse from a high-voltage power supply. The Boomer pulse provided good repeatability and a broad spectrum between 400 Hz and 7000 Hz (Donda et al., 2008). The streamer is pre-amplified and consists of ten hydrophones with high sensitivity and a bandwidth of 100 Hz to 10 kHz that stack signals without normal move out (NMO) correction. Depending on the water depth, the hydrophones can be interchanged by closing some of them. Data were collected using a parallel geometry (Baradello and Carcione, 2008). In this geometry, the streamer and the seismic source were towed at the same distance from the Zodiac boat (10 m).

The seismic data (all D-GPS navigated), were recorded with the Seismodule Controller Software (SCS; Geometrics) in SEGY format with a window length of 400 ms, a variable time delay depending on lake floor position, and a sampling rate of 50 μs. The acquisition interval was 0.5 s at an average boat speed of 4 knots. NavPro (Communication Technology) software was used on a laptop to plan and track the routes.

After amplification (spherical divergence and inversion curve) and filtering (DC -removal and bandpass filter), an algorithm consisting of creating common-offset gathers and transforming them to the time-frequency domain within short windows using the Fast Fourier Transform was used to eliminate the electrical noise. To increase the vertical resolution and improve the signal-to-noise ratio, a deconvolution based on a Wiener-Levinson filter was used.

For the two-way travel time (TWT) to depth conversion of seismic sections, an average sound velocity of 1650 m/s was used for the glaciolacustrine sediment, based on the velocity analysis of Lozano et al. (2020) for Brazo Rico and Brazo Sur. A sound velocity of 1432 m/s was used for the water column (Zanolla et al., 2011).

3.2. Identification and interpretation of the seismic sequences

The analysis of the seismic records was carried out according to the concepts of seismic stratigraphy (Catuneanu, 2006). As a first step, seismic facies were identified based on seismic attributes such as amplitude, continuity, termination, intensity, and geometry of the reflections. These seismic facies can be interpreted as the result of different sedimentary processes. In addition, seismic units were defined as broad parts of the seismic section based on geometric patterns, architecture, and stratigraphic relationships that are bounded by unconformities. These units were interpreted with respect to the sedimentary environment. This methodology has been applied in other lakes in Patagonia (Esteban et al., 2014; Lozano et al. 2018a, 2018b, 2021a; Bran et al.,
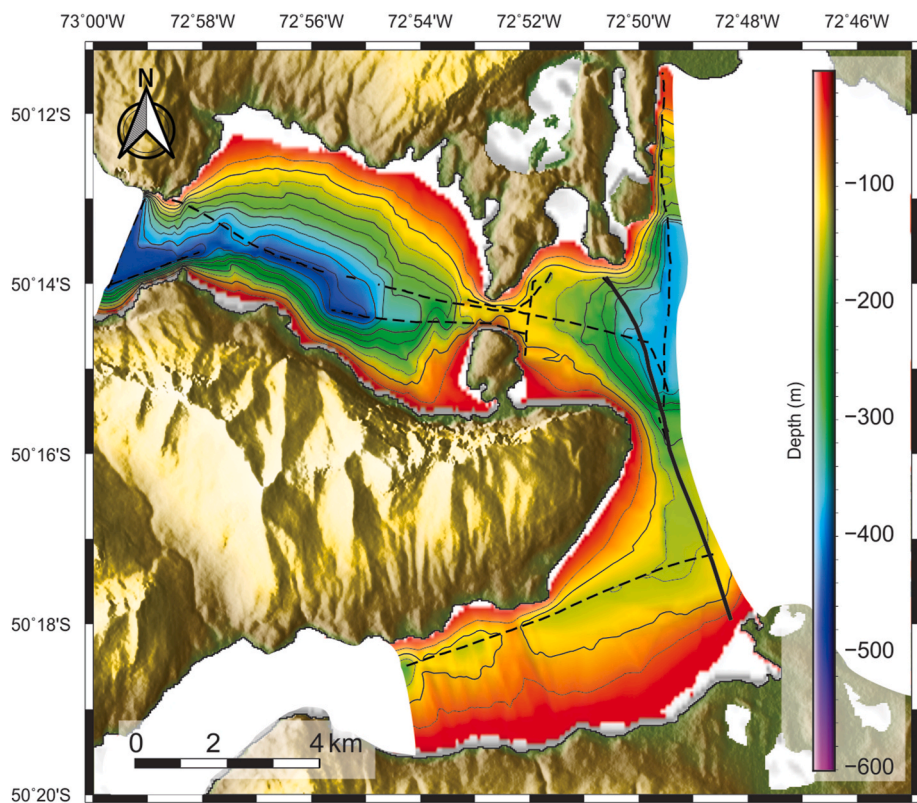
Fig. 3. Bathymetric map of the northern area of Punta Bandera. The dashed black lines mark the seismic survey locations. The thick red line is the full, high-resolution seismic section shown in Fig. 5. White areas lacks of bathymetry data.

2019), Switzerland (Fabbri et al., 2018), and especially in other areas of Lago Argentino (Lodolo et al. 2020a, 2020b; Lozano et al., 2020c, 2021b).

To analyze the sedimentation processes in the uppermost sediment layer of Lago Argentino, images of gravity cores taken from the open database (https://zenodo.org/record/5815107) of Van Wyk de Vries et al. (2022) were used. The location is shown in Fig. 2.

4. Results

4.1. Morphology of the lake floor

We derived information about the depth of the lake floor from the seismic records to create a grid. The reflections from the lake floor were converted to depth values, and then combined with the topography of the surrounding areas of the lake arm to create a more reliable model of the grid developed. This approach reduced the occurrence of artifacts in the grid calculation.

The resulting bathymetry is shown in Fig. 3. The model only includes the areas where seismic lines were actually recorded. The morphology of the lake floor can be divided into two main zones: the northern area of the Brazo Norte and the southern area of the Canal de los Témpanos, the latter being shallower than the former. The two levels of the lake floor can be seen directly in the seismic section in Fig. 5. This overdeepening of the Brazo Norte glacial valley represents the most notable feature of the bathymetric grid, and is discussed later in section 5.4.

The southern area, the easternmost part of the Canal de Los Témpanos, has a maximum depth of 160 m. It is divided into two areas separated by a morphological elevation at 72°52' W.

The northern area of the Brazo Norte is deeper and reaches almost 500 m in the middle of the lake arm. Near the narrow strait of Boca del Diablo, the lake floor is shallower and reaches a depth of 120 m.

The easternmost seismic lines have recorded a maximum depth of

400 m in the direction of the main body of Lago Argentino. However, it is likely that the depth increases towards the east.

The slopes are different on both sides of the arms of the lake. Near Punta Bandera the slope is almost 5°, while at Punta Avellaneda it is steeper at 9°. In Brazo Norte, the slopes are steeper, reaching more than 70° in the area of Boca del Diablo, while on the northern slope they average 24° and on the southern slope 11°.

4.2. Description of the seismic stratigraphy

Eight seismic facies were recognized in the seismic record of the northern area of Punta Bandera. These seismic facies were defined based on their seismic characteristics such as amplitude of reflections, continuity, transparency, geometry and termination of the reflections. The seismic facies are: (i) chaotic facies (CSF); (ii) mound facies (MSF); (iii) chaotic facies with diffraction (CDSF); (iv) prograding facies (PSF); (v) high amplitude parallel facies (HASF); (vi) divergent facies (DVSF); (vii) gas facies (GSF); (viii) low amplitude parallel facies (LASF). Fig. 6 provides an overview of the characteristics of the individual seismic facies.

The seismic facies are grouped into two main seismic units distributed over the seismic sections. The older seismic unit is the lower unit (PB-LU), which overlies the acoustic basement and is located exclusively in the southern part of the section (Fig. 5). The thickness of this unit in the area of the seismic section reaches 0.055 TWT (~44 m using 1650 m/s for time to depth conversion; Lozano et al., 2020). It is composed of the CDSF and MSF seismic facies.

The upper unit (PB-UU) includes a variety of seismic facies that dominate the sedimentary fill in this area of Lago Argentino. It is composed of the seismic facies PSF, HASF, LASF, and DVSF seismic facies, with HASF and LASF dominating. The main feature of this seismic unit is its layered and continuous reflections, which differ from the PB-LU reflections. The thickness of the unit is variable, but reaches a maximum of 0.066 TWT (~53 m at 1650 m/s) in the deepest basin on
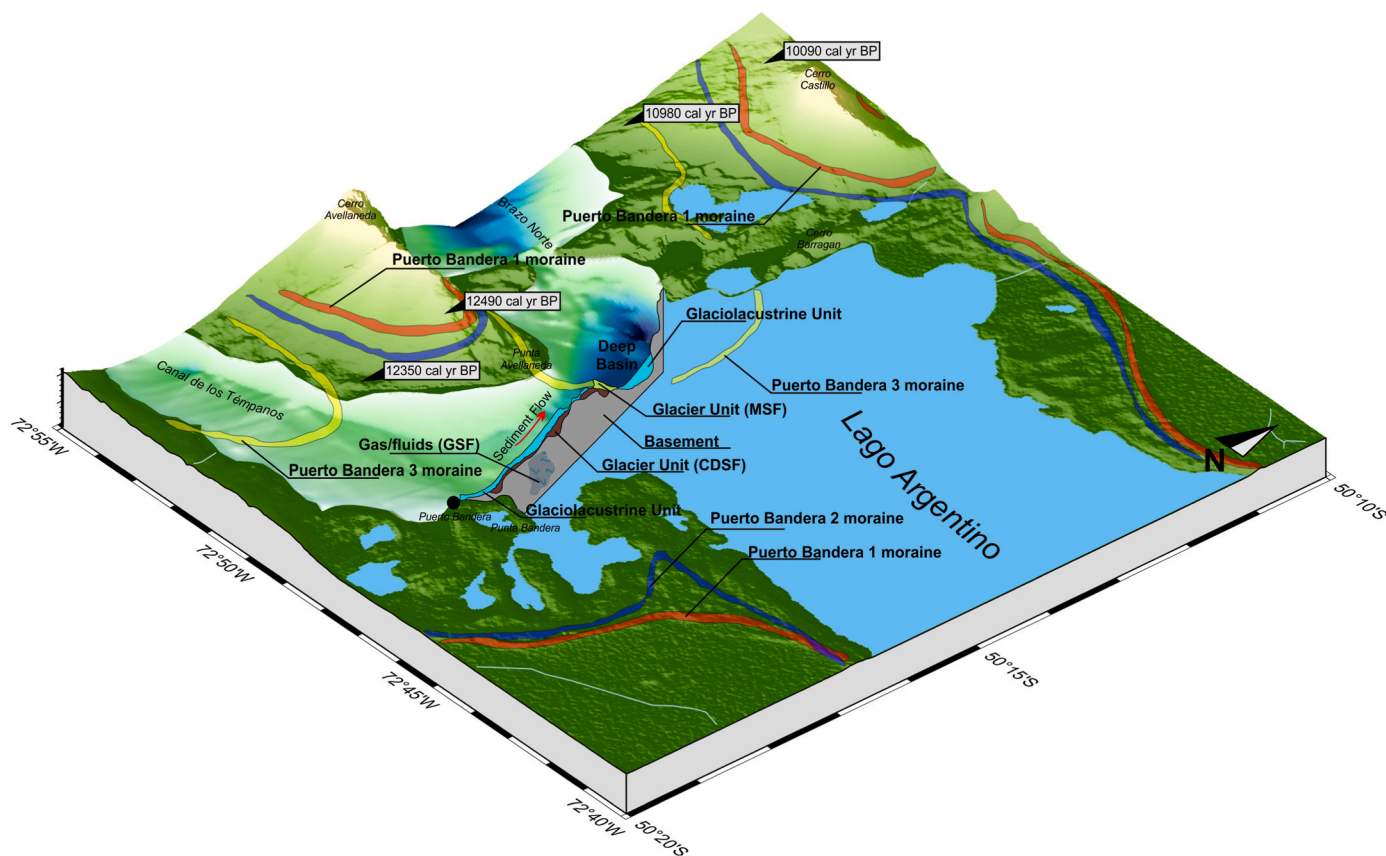
Fig. 4. 3-D block diagram of the bathymetry of the Canal de los Témpanos and the Brazo Norte of Lago Argentino at Punta Bandera. The age data are from Strelin et al. (2011).

the north side. The thickness is similar above the central basin and decreases towards the south.

4.3. Unconformities

Some unconformities were recognized in the seismic record. These surfaces are shown in the seismic sections with colored lines (Fig. 5). The unconformities represent a change between the underlying and overlying seismic reflections in the form of an erosive truncation, a transition from parallel to divergent reflections, a significant change in amplitudes, or some other feature.

Ten unconformities were defined, labeled U1 to U4 and U5.1 to U5.6. The last six unconformities represent some minor changes that are interpreted as minor variations in depositional and/or erosional processes compared to U1 to U4.

A summary of the most important features of the unconformities is shown in Fig. 7.

5. Discussion

5.1. Seismic facies interpretation

Seismic facies can be analyzed and interpreted as the result of a specific sediment type and depositional processes. Fig. 6 provides a summary of the individual seismic facies with the corresponding interpretation.

The CSF is the acoustic basement. As no other deeper and defined reflections are visible in it, it is interpreted as the bedrock of the lake. The stratigraphy of the Punta Bandera area is characterized by outcrops of the Cretaceous Cerro Toro and Rio Mayer formations, which consist of mudstones, sandstones, and turbidites (Nullo et al., 2006). The Upper

Jurassic El Quemado Complex also outcrops and consists of volcanics, sandstones, and mudstones (Nullo et al., 2006). The seismic record does not allow us to distinguish between these lithologies based on different seismic attributes, so we cannot determine the specific rock type that makes up the bedrock.

CDSF is considered to be one of the main components of PB-LU. Based on the seismic attributes and characteristic morphology, these can be interpreted as glacial deposits, such as glacial diamicton. The MSF is quite similar to the CSSF, but has lower amplitude and transparency than the latter. This type of seismic facies has already been interpreted in other sectors of Lago Argentino, so it is widespread in this area (e.g., Lodolo et al., 2020a, b; Lozano et al., 2020c, 2021b, 2022). In addition, seismic facies with the same characteristics and morphology have been identified in other Patagonian lakes such as Lago Yeuhin, Chepelmut, and Fagnano (e.g., Lozano et al., 2018a, b, 2021a).

The PB-UU consists of the majority of the facies recognized in the seismic record. HASF, LASF, and DVSF have already been interpreted in the southern arms of Lago Argentino (Lozano et al., 2021b), with the high-amplitude reflections of HASF being assigned to coarser clastic particles. The coarser sediments can be associated with sandy layers recognized in sediment cores (Fig. 8A–F, I). These layers are located above erosive surfaces (Fig. 8D, E, H, J) and may be the result of a flow deposits, such as underflows or turbidity currents. Normal gradations of these deposits are observed in sediment cores (Fig. 8F–I).

LASF is a seismic facies interpreted as a hemipelagic layer composed of water column sediments (silt, clay, and biogenic particles, Fig. 8B). Layered sediments (Fig. 8A–E) in the sediment cores were analyzed and interpreted as varves (Van Wyk de Vries et al., 2022).

DVSF are divergent reflections that can be considered as advancing clinoforms and interpreted as clastic fan deltas. This seismic facies is restricted to the slope fault (Fig. 5 E). PSF is similar to DVSF, with the
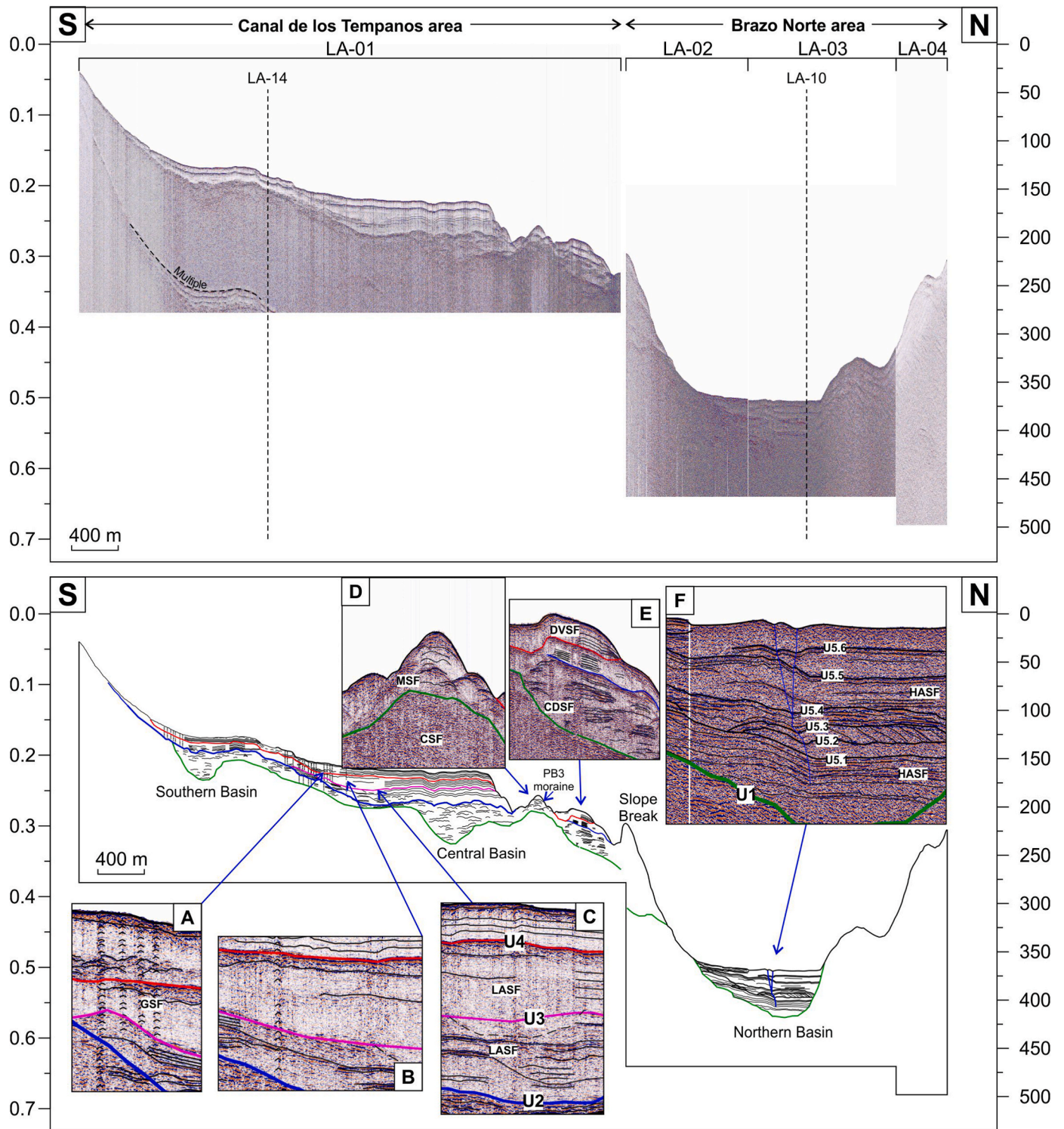
Fig. 5. N–S composite seismic profiles. Top: the uninterpreted section. Bottom: a line drawing showing the main reflections, unconformities, and faults. The insets from A to F highlight particular features of the seismic facies and/or unconformities, which are described in detail in the text.

diference that the reflections have larger amplitude and are more tilted northward. The processes are interpreted in the same way, namely as a clastic fan delta, but with a different distance of sediment input. The depth of the basin may have also acted differently in the same process, resulting in DVSF for shallow water and PSF for deep water. The sedimentation processes that take place during in the deposition of clastic fan deltas differ from those of the hemipelagic drape. They can be traced by means of sedimentary structures in sandy strata, such as cross-bedding strata (Fig. 8C).

The last seismic facies is the GSF (Fig. 5A) and, as early mentioned, is characterized by the occurrence of blanking effects, possibly due to the presence of gas or fluids. A similar facies has been detected with the same acoustic signature in other Patagonian lakes such as Lago Fagnano (e.g., Lodolo et al., 2012).
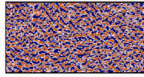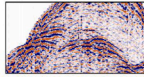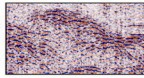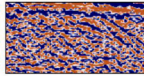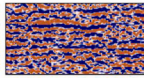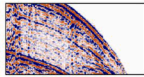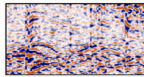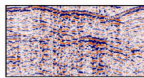
Seismic Facies	Example	Description	Interpretation
CSF chaotic facies		Chaotic, discontinuous seismic facies. No internal arrangement.	This facies is interpreted as the acoustic basement, and may be related with the bedrock below the sedimentary infill of the lake.
MSF mound facies		Mounded morphology, transparent areas and a few diffractions were recognized. The maximum thickness of the seismic facies is up to 0.04 TWT (~22 m)	It is interpreted as an exposed moraine deposits, included in the glacier unit. It is composed by coarse to fine grain sediment of glacial diamicton.
CDSF chaotic with diffraction facies		High amplitude and curve reflections forming globular morphologies. The maximum thickness of the facies is almost 0.05 TWT (~38 m).	This seismic facies is included in the glacier unit, underlying the glaciolacustrine unit. It is interpreted as till deposits, composed of coarse to fine grain sediment of glacial diamicton.
PSF progradant facies		Bounded between the HASF, has a maximum thickness of 0.015 TWT (10 m). It is composed by divergent reflections that dip northwards.	The layered, divergent reflections of this seismic facies are essentially prograding clinoforms. They are interpreted as clastic fan deltas.
HASF high amplitude parallel facies		Parallel, continuous and high amplitude reflections. This facies is widely distributed in the seismic record.	This facies is interpreted as laminated draping deposits. The high-amplitude reflections can be caused by coarser terrestrial particles.
DVSF divergent facies		It has similar characteristics with the HASF but the reflections are divergent northwards. The maximum thickness is 0.015 TWT (~10 m).	This seismic facies is characterized by a wedge geometry northwards, which is interpreted as a distal part of a clastic fan delta.
GSF gas facies		Discontinuous reflections with small diffractions that are stacked vertically. It appears overprinted to the other seismic facies in the southern and central basins	Interpreted as a disturbance of the deposits due to the presence of gas within the sediments.
LASF low amplitude parallel facies		Parallel, continuous and low amplitude seismic facies. Sometimes transparent zones are observed.	Interpreted as hemipelagic drape. This consists in draping sediments of the water column like silt, clay and biogenic particles.

Fig. 6. Seismic facies identified in the seismic record. The interpretation of each facies is shown on the right hand side.

5.2. Seismic units interpretation

PB-LU is interpreted as a unit composed of glacial deposits such as till. The same seismic features recognized in the seismic facies, CDSF and MSF, were also present in the Brazo Rico and Brazo Sur glacial seismic units (Lozano et al., 2021b). The typical mound morphology, flexure, and distribution across bedrock have also been interpreted in other periglacial lakes (e.g., Waldmann et al., 2008, 2010a, b).

PB-UU represents glaciolacustrine sedimentation after ice retreat in the lake basin. The parallel, continuous reflection arrangement and the draping distribution are the typical and most important features of this type of sedimentation. The same sedimentation is widespread in the different arms of Lago Argentino (Lodolo et al. 2020a, 2020b; Lozano et al., 2021b, 2022; Caffau et al., 2022).

5.3. Glacial advances and retreat

Moraine deposits on land have been recognized in the Lago Argentino area by several authors (e.g., Strelin et al., 2011, 2014; Kaplan et al., 2011, 2016). Some of the morphologies identified in the seismic records have been correlated with onshore deposits based on morphological features and/or proximity between features. The aim of this correlation is to address the lack of temporal assignments so that most of the events described below are included in a hypothetical model (Fig. 9).

The glaciation history in the Punta Bandera area is well documented on land by the presence of several moraine deposits at Punta Avellaneda (Fig. 4; Strelin et al., 2011, 2014; Kaplan et al., 2011). These moraines correspond to the Late Glacial Puerto Bandera 1, 2, and 3 moraines (PB1, PB2, and PB3). The ages determined from a peat bog in the Punta Avellaneda sector indicate that moraine PB1 (Fig. 9A) retreated prior to 12,490 cal yr BP ± 80 yr and the retreat of moraine PB2 (Fig. 9B)

occurred more than 12,350 cal yr BP ± 120 yr (1σ error; Strelin et al., 2011). Moraine PB3 is younger than the earlier moraines, and considering that the peat bog at Bahía Catalana was ice-free for more than 12, 280 cal yr BP ± 110 yr (Strelin et al., 2011), the ice must have retreated several kilometers in less than 70 years.

The location of the Puerto Bandera 3 moraine on land is consistent with the location of the mounded morphology of the MSF seismic facies (Fig. 5D). Therefore, it can be reasonably interpreted that this seismic facies and this sector of the PB-LU coincide with the Puerto Bandera 3 moraine identified by Strelin et al. (2011). From this point, we can make some considerations about sedimentation in the basins during glacial retreat (Fig. 9D).

Since PB-LU is sediments deposited by glacial retreat (Fig. 9C) and PB3 is the younger moraine of the Puerto Bandera moraines, the seismic facies CDSF contained in PB-LU could correspond to an older glacial retreat. Therefore, the glacial deposits in the southern sector of the profile, in the Canal de Los Témpanos area, are older than the PB3 moraine (MSF in Fig. 5).

It can be hypothesized that the unconformities developed in the same way as in the southern arms of Lago Argentino (Lozano et al., 2021b). The main driving force for the development of these surfaces was density currents and mass-wasting processes, controlled by the energy level in the environment (Lozano et al., 2021b). During glacier front fluctuations, the energy fluctuated and led to a drastic change in sediment dynamics. Low energy phases may correspond to ice front stagnation phases, while high energy phases correlate with ice front retreat. With higher water and sediment input during a retreat phase, the occurrence of density currents and thus the development of erosional surfaces would be more frequent.

The U2 unconformity represents a change in the sedimentation processes. The sediments below the U2 layer consist exclusively of

Surface	Description
U1	Unconformity that separates the acoustic basement from the overlying units. Clearly visible in the entire section (Figure 3). Morphology characterized by small basins and sills. Basins above U1 in the southern area are filled with PB-LU. In the deeper northern area, the basin is filled with seismic layered facies contained in the PB-UU.
U2	Unconformity (Figure 3C) that separates the glacier deposits from the glaciolacustrine sediments. It is recognized only in the southern shallow area. It is characterized by a sharp change in seismic properties of the reflections from CDSF to HASF.
U3	An erosive truncation (Figure 3C) that is observed mostly in the shallow part of the seismic record, and disappears to the north.
U4	It is located only in the southern area, and is characterized by an erosional truncation (Figure 3C). Next to the slope break, the unconformity represents a change in the seismic reflection from parallel (below) to divergent (above).
U5.1 to U5.6	Small unconformities restricted to the deep basin of the northern area. Represent changes in the reflection geometry. It is composed by a total of six small surfaces (Figure 3F). U5.1 separates parallel reflections with reflections above that terminates against the unconformity with a geometry similar to downdip. U5.2 and U5.3 bound a package of northward dipping reflections. U5.4 shows erosional truncation on the north side of this basin and also has a sequence of high and continuous amplitude reflections at the bottom (HASF) and parallel low amplitude reflections at the top (LASF). U5.5 resembles U5.4 with erosional trunctaion, but separates two packages of LASF bounded by a high amplitude reflection. U5.6 is the younger unconformity on the north side of the section, and has same features as U5.5.

**Fig. 7.** Summary of unconformities identified in the seismic record.

glacial deposits, while sedimentation above the unconformity consists of glaciolacustrine (PB-UU). The minimum age for the ice retreat of Península Avellaneda dated by Strelin et al. (2011) gives us clues for a preliminary age assignment for U2. The retreat of PB1 (12,490 cal yr BP) and of PB2 (12,350 cal yr BP) coincides with a time when the Canal de los Témpanos area was covered by ice. Therefore, glaciolacustrine sedimentation began there, and the U2 unconformity can be placed between these ages (Fig. 10). The estimated age of U2 is consistent with the age determined for the onset of glaciolacustrine sedimentation in the southern arms of Lago Argentino, Brazo Sur, and Brazo Rico, namely 12.6 ± 0.7 cal kyr BP (Lozano et al., 2021b).

During the stabilization phase, when the PB3 moraine formed, the Brazo Norte area remained covered by ice. However, the shallower area of the Canal de los Témpanos was exposed. Glacial sedimentation is thought to have started first in this shallow area, and the first reflections at PB-UU show a time interval that is not present in the northern basin, the Brazo Norte area. After the glacial retreat of PB3, glacial sedimentation continued in both the southern and northern areas.

It is believed that there are indicators or clues in the seismic record

that suggest two sedimentation phases in the Canal de los Témpanos area. The first stage corresponds to sedimentation during the stabilization phase of PB3 (Fig. 9D), with a very close location of the ice front; a late stage with a distal ice front after the glacial retreat in Brazo Norte. The unconformities recognized in the Canal de los Témpanos area show a differentiation of the records of PB-UU. The older unconformity within PB-UU (U3) separates two packages of LASF. This slightly eroded surface may indicate the period when the ice front retreated after the deposition of PB3 (Fig. 9E).

In Brazo Sur and Brazo Rico, two erosional unconformities labeled BR -U3 and BS –U2 were correlated and assigned a relative time. The strong erosional signature and location near the top of the sediment fill were similar, and a middle Holocene age was determined (Lozano et al., 2021b). This age corresponds to a glacial advance that is between 6.1 and 5.7 kyr BP (Strelin et al., 2014; Kaplan et al., 2016). The unconformities were formed during the retreat that followed the glacial advance. The U4 unconformity is only found in the shallow southern part of the Canal de los Témpanos, and the similarity with the above-mentioned unconformities in the southern arms of Lago
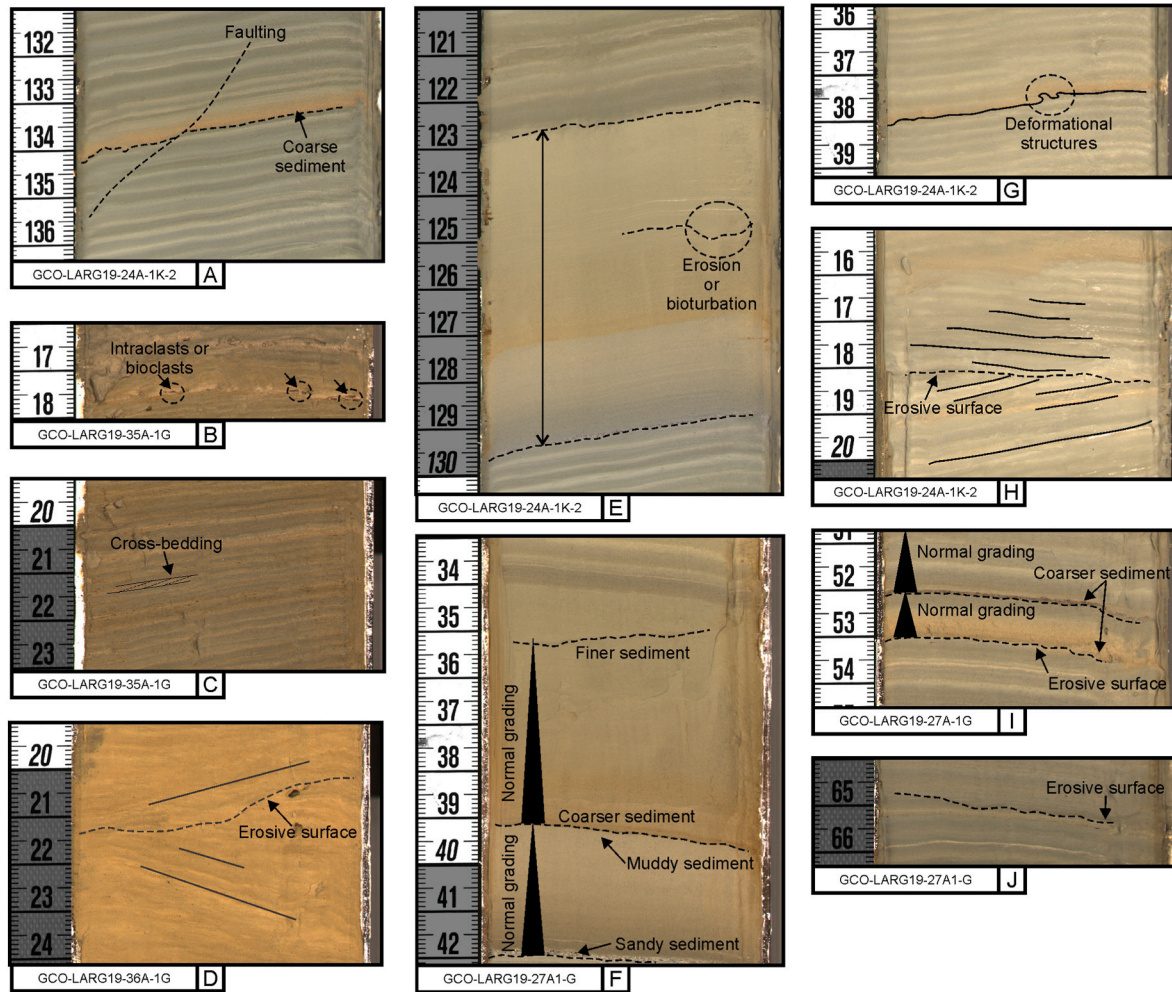
Fig. 8. Sections from GCO-LARG19 27, 24, 35, and 36 gravity cores. Examples are from the Van Wyk de Vries et al. (2022) open database (https://zenodo.org/record/5815107). The interpretation was carried out for this work. The location is shown in Fig. 2.

Argentino is obvious. We can tentatively associate the same event with U4 and assign an age between 6.1 and 5.7 years to the unconformity (Fig. 10).

The unconformities in the Brazo Norte area, in the northern basin, are more difficult to assign. Because the basin is deeper than the central and southern basins (Fig. 5), the internal arrangement of deposits reflects less environmental change than the shallower deposits. Five glacial advances were recorded after the 5.7 kyr BP (Strelin et al., 2014). We can tentatively link these advances to the development of the six unconformities in the northern basin, but the mechanism and timing of the events remain speculative.

5.4. Considerations on the morphology of the lake floor

The morphology of the Canal de los Témpanos and the Brazo Norte shows a clear difference in depth, which indicated that the two valleys developed differently during the glacial activity. The overdeepening of the Brazo Norte is a special feature in which several parameters may have played a role. Overdeepening of glacier beds is to be expected because the pattern of ice flow, which largely determines largely the pattern of basal sliding, should result in the erosion and sediment transport potential peaking at a location close to the long-term average height of the equilibrium line (Cook and Swift, 2012). Some studies suggest that overdeepening is promoted by changes in the geologic structure or lithology; these may initially lead to small irregularities in the subsurface that are amplified by feedbacks between

ice-water-erosion and may coalesce into a single graded overdeepening (Swift et al., 2008; Jordan, 2010; Preusser et al., 2010).

Three main hypotheses can be considered to explain the different depths. The first is related to the glacier volume. The lobe of the Brazo Norte could be thicker than the lobe of the Canal de los Témpanos and therefore have cut deeper on the northern side than on the southern side. The second hypothesis refers to structural control, in which the northern side was mainly developed deeper, possibly due to the presence of an E-W fault zone, and consequently more was excavated in the northern area than in the southern one. The third hypothesis relates to the lithological control, according to which the northern area was more susceptible to glacial erosion due to the lower resistance of the rock to glacial flow. The geologic map of the area (see Nullo et al., 2006, Fig. 1) shows that the El Quemado complex occurs at the northern margin of Lago Argentino and consists of volcanic rocks, sandstones, and mudstones. However, the distribution of the El Quemado complex in the bedrock of the lake is not yet clear. Looking at the retreat of the Puerto Bandera moraines (Fig. 9), it can be seen that the northern glacier is retreating somewhat more slowly than the southern glacier. This could be due to the thickness of the two glaciers, with the thicker northern glacier creeping in the deep area of the Brazo Norte, while the southern, thinner glacier calves in the area of the Canal de los Témpanos due to its uplift. The most likely hypothesis is therefore the first, in which the different thickness of the northern and southern ice lobes cause the differences in the depth of the two valleys. Overdeepening valleys and basins are common in the alpine region. Glacier flow, which is controlled by mass balance and ice
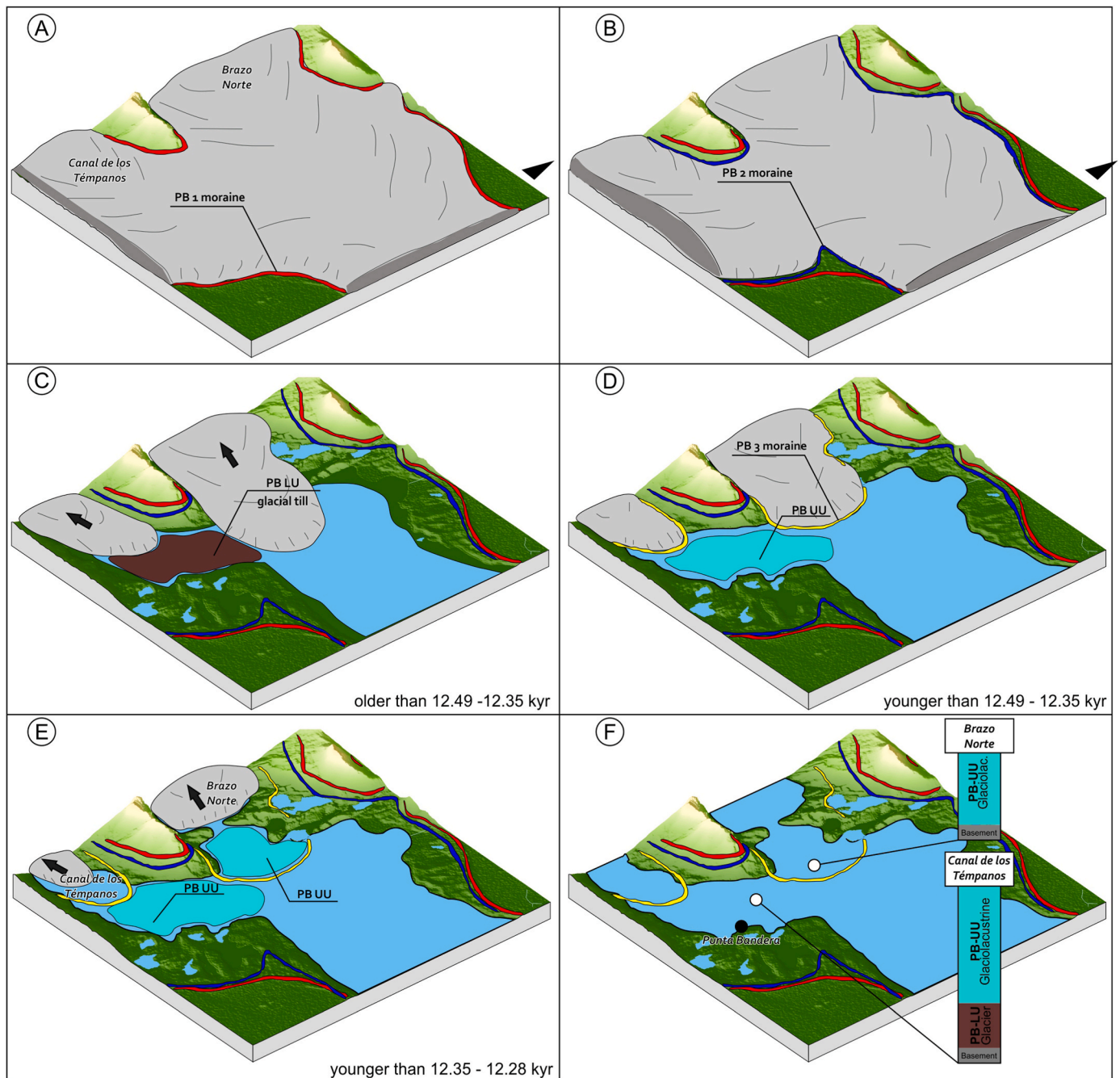
Fig. 9. Evolutionary scheme proposed for the area. A. Evolution of the PB1 moraine. B. Evolution of the PB2 moraine. C. Retreat of the northern and southern ice lobes. In this phase, PB-LU is deposited over the basement in the Canal de los Témpanos. D. Evolution of the PB3 moraine and deposition of PB-UU (glaciolacustrine) in the Canal de los Témpanos. E. Retreat of the northern and southern lobes and deposition of PB-UU (glaciolacustrine9) in the Canal de los Témpanos and Brazo Norte. F. Punta Bandera area as present-day setting.

dynamics, is considered an important factor in the formation of over-deepening (Preusser et al., 2010). This could be the case. However, these features have not yet been recognized in other lakes on the eastern side of the SPI. This is because information on the water bodies is sparse, and bathymetric data can only be found for very small areas, generally near the glacier fronts (i.e. Skvarca et al., 2002; Zamorano Morales, 2020).

6. Conclusions

The seismic survey carried out in the studied area made it possible, for the first time, to produce of a bathymetric map of the northern Punta Bandera area in Lago Argentino. The area is divided into two sectors: a

northern, overdeepened area and a southern, shallower area, each with different morphologies. The differences in depths between both lake arms may be due to different thicknesses of the ice lobes during the deglaciation time.

Several seismic facies have been identified in the seismic profiles. Two of these seismic facies have been combined into one seismic unit, interpreted as of glacial in origin, consisting of bedload deposits, and named PB-LU. This unit lies above the bedrock of the lake and is located in the shallower, southern part of the Canal de los Témpanos. The other five seismic facies are contained in an upper seismic unit labeled PB-UU, which is interpreted as a glaciolacustrine deposit. These deposits are distributed throughout the northern and southern areas.
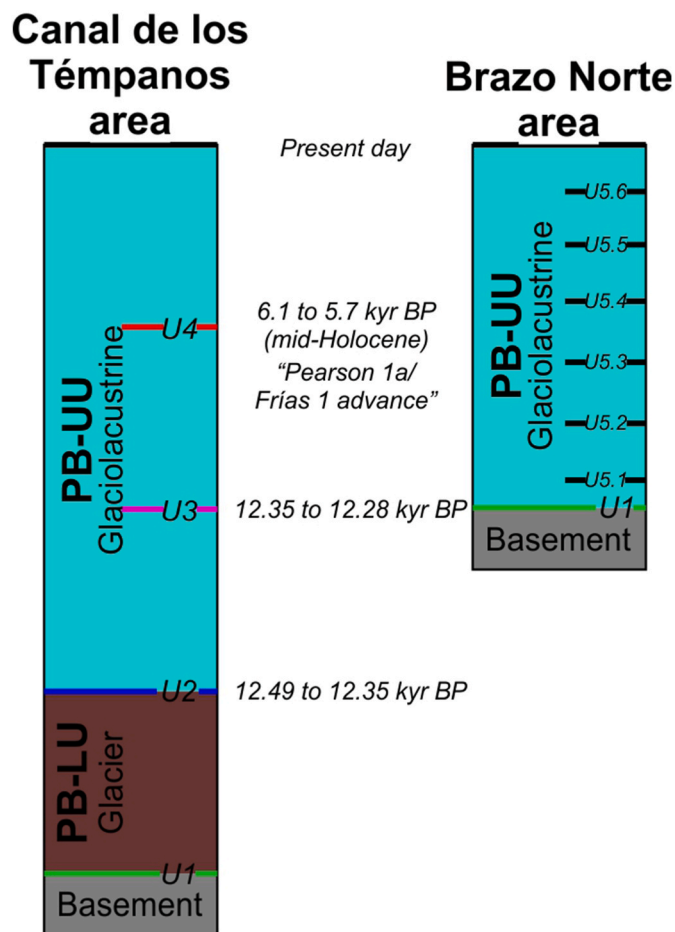
Fig. 10. Relative ages for the unconformities in the southern and northern parts of the study area. The data used for the correlation are based on Strelin et al. (2011, 2014) and Kaplan et al. (2011, 2016).

The seismic facies MSF has been correlated with the Puerto Bandera 3 continental moraine. The continuation of the land moraine arc in the lake floor is consistent with the mound morphology observed in the seismic sections.

The erosional unconformities observed in the shallower part of the Canal de los Témpanos are evidence of the different retreats of the Puerto Bandera moraines. After the retreat of the glacier front from the moraine deposits, the water inflow caused turbidity currents that eroded the sediments in the basins and allowed the formation of unconformities.

According to the proposed model for deglaciation in the Punta Bandera area, the southern, shallower area of the Canal de los Témpanos was free from ice earlier than the northern, overdeepened zone of the Brazo Norte. The accumulation of sediment in areas occurred at different times and represents phases in which the ice front was divided into two lobes that retreated to the west.

Data availability

Data used for the manuscript will be available on request.

CRediT authorship contribution statement

Jorge G. Lozano: Conceptualization, Investigation, Methodology, Software, Visualization, Writing – original draft, Writing – review & editing. **Florencia B. Restelli:** Software, Visualization, Writing – review & editing. **Stefania Bunicontro:** Writing – review & editing. **Salomé C.** **Salvó Bernárdez:** Investigation, Methodology, Visualization, Writing – review & editing. **Donaldo M. Bran:** Methodology, Software, Visualization, Writing – original draft, Writing – review & editing. **Maurizio Grossi:** Funding acquisition, Methodology. **Emanuele Lodolo:** Funding acquisition, Project administration, Supervision, Writing – review & editing. **Alejandro A. Tassone:** Funding acquisition, Project administration, Supervision, Writing – review & editing.

Declaration of competing interest

The authors declare that they have no known competing financial interests or personal relationships that could have appeared to influence the work reported in this paper.

References

Alley, R.B., Cuffey, K.M., Evenson, E.B., Strasser, J.C., Lawson, D.E., Larson, G.J., 1997. How glaciers entrain and transport basal sediment: physical constraints. Quat. Sci. Rev. 16, 1017–1038.

Baradello, L., Carcione, J.M., 2008. Optimal seismic-data acquisition in very shallow waters: surveys in the Venice lagoon. Geophysics 73 (6), 59–63.

Bran, D.M., Lozano, J.G., Civile, D., Lodolo, E., Cerredo, M.E., Tassone, A., Baradello, L., Grossi, M., Vilas, J., 2019. Post-Last Glacial Maximum evolution of a "fjord-type" lake based on high-resolution seismic data: the Lago Roca/Acigami (southern Tierra del Fuego, Argentina/Chile). J. Quat. Sci. 35 (3), 396–409. https://doi.org/10.1002/jqs.3179.

Caffau, M., Lodolo, E., Donda, F., Zecchin, M., Lozano, J.G., Nasi, F., Bran, D.M., Tassone, A., Caburlotto, A., 2022. Stratigraphic signature of the Perito Moreno ice-dammings during the Little ice age (southern Patagonia, Argentina). Holocene 32 (3), 174–182. https://doi.org/10.1177/09596836211060496.

Calcagno, A., Fioriti, M., Pedrozo, F., Vigliano, P., López, H.L., Rey, C., Razquin, A.M., Quirós, R., 1995. Catálogo de lagos y embalses de la Argentina. ARM & Asociados.

Caldenius, C.R.C., 1932. Las glaciaciones cuaternarias en la Patagonia y Tierra del Fuego: una investigación regional, estratigráfica y geocronológica, una comparación con la escala geocronológica sueca. Geografiska Annaler 14 (1–2), 1–164. https://doi.org/10.1080/20014422.1932.11880545.

Catuneanu, O., 2006. Principles of Sequence Stratigraphy, first ed. Elsevier, Amsterdam.

Cook, S.J., Swift, D.A., 2012. Subglacial basins: their origin and importance in glacial systems and landscapes. Earth Sci. Rev. 115 (4), 332–372.

Coronato, A., Rabassa, J., 2011. Chapter 51 - Pleistocene Glaciations in Southern Patagonia and Tierra del Fuego. In: Jürgen Ehlers, P.L.G., Philip, D.H. (Eds.), Developments in Quaternary Sciences. Elsevier, pp. 715–727.

Davies, B.J., Glasser, N.F., 2012. Accelerating recession in Patagonian glaciers from the "Little ice age" (c. AD 1870) to 2011. J. Glaciol. 58, 1063–1084.

Davies, B.J., Darvill, C.M., Lovell, H., Bendle, J.M., Dowdeswell, J.A., Fabel, D., García, J.-L., Geiger, A., Glasser, N.F., Gheorghiu, D.M., Harrison, S., Hein, A.S., Kaplan, M.R., Martin, J.R.V., Mendelova, M., Palmer, A., Pelto, M., Rodés, A., Sagredo, E.A., Smedley, R.K., Smellie, J.L., Thorndycraft, V.R., 2020. The evolution of the Patagonian Ice Sheet from 35 ka to the present day (PATICE). Earth Sci. Rev. 204, 103152.

Donda, F., Brancolini, G., Tosi, L., Kovačević, V., Baradello, L., Gačić, M., Rizzetto, F., 2008. The ebb-tidal delta of the Venice Lagoon, Italy. Holocene 18 (2), 267–278. https://doi.org/10.1177/0959683607086765.

Esteban, F.D., Tassone, A., Lodolo, E., Menichetti, M., Lippai, H., Waldmann, N., Darbo, A., Baradello, L., Vilas, J.F., 2014. Basament geometry and sediment thickness of Lago Fagnano (Tierra del Fuego). Andean Geol. 41 (2), 293–313.

Fabbri, S.C., Buechi, M.W., Horstmeyer, H., Hilbe, M., Hübscher, C., Schmelzbach, C., Weiss, B., Anselmetti, F.S., 2018. A subaquatic moraine complex in overdeepened Lake Thun (Switzerland) unravelling the deglaciation history of the Aare Glacier. Quat. Sci. Rev. 187, 62–79.

Ghiglione, M.C., Suarez, F., Ambrosio, A., Da Poian, G., Cristallini, E.O., Pizzio, M.F., Reinoso, R.M., 2009. Structure and evolution of the Austral basin fold-thrust belt, southern patagonian Andes. Rev. Asoc. Geol. Argent. 65 (1), 215–226.

Glasser, N., Jansson, K., 2008. The glacial map of southern south America. J. Maps 4, 175–196.

Glasser, N.F., Jansson, K.N., Harrison, S., Kleman, J., 2008. The glacial geomorphology and Pleistocene history of South America between 38°S and 56°S. Quat. Sci. Rev. 27, 365–390.

Glasser, N.F., Jansson, K.N., Duller, G.A.T., Singarayer, J., Holloway, M., Harrison, S., 2016. Glacial lake drainage in Patagonia (13-8 kyr) and response of the adjacent Pacific Ocean. Sci. Rep. 6, 21064.

Gourlet, P., Rignot, E., Rivera, A., Casassa, G., 2016. Ice thickness of the northern half of the Patagonia Icefields of South America from high-resolution airborne gravity surveys. Geophys. Res. Lett. 43, 241–249.

Jordan, P., 2010. Analysis of overdeepened valleys using the digital elevation model of the bedrock surface of Northern Switzerland. Swiss J. Geosci. 103, 375–384.

Kaplan, M.R., Strelin, J.A., Schaefer, J.M., Denton, G.H., Finkel, R.C., Schwartz, R., Putnam, A.E., Vandergoes, M.J., Goehring, B.M., Travis, S.G., 2011. In-situ cosmogenic 10Be production rate at Lago Argentino, Patagonia: implications for lateglacial climate chronology. Earth Planet Sci. Lett. 309, 21–32. https://doi.org/10.1016/j.epsl.2011.06.018.

Kaplan, M., Schaefer, J., Strelin, J., Denton, G., Anderson, R., Vandergoes, M., Finkel, R., Schwartz, R., Travis, S., Garcia, J., 2016. Patagonian and southern south atlantic view of Holocene climate. Quat. Sci. Rev. 141, 112–125.

Kilian, R., Lamy, F., 2012. A review of Glacial and Holocene paleoclimate records from southernmost Patagonia (49-55°S). Quat. Sci. Rev. 53, 1–23.

Kraemer, P.E., Ploszkiewicz, J.V., Ramos, V.A., 2002. Estructura de la Cordillera Patagónica Austral entre los 46 y 52 S. In Geología y Recursos Naturales de la provincia de Santa Cruz. Relatorio del 15 Congreso Geológico Argentino, El Calafate, Santa Cruz, Asociación Geológica Argentina 353–364.

Lippai, H., Lodolo, E., Tassone, A., Hormaechea, J.L., Menichetti, M., Vilas, J.F., Tesac, Party, 2004. Morpho-structure of Lago Fagnano (Tierra del Fuego) and adjacent areas. Boll. Geofis. Teor. Appl. 45 (2), 142–144.

Lodolo, E., Menichetti, M., Tassone, A., Geletti, R., Sterzai, P., Lippai, H., Hormaechea, J.L., 2002. Researchers target a continental transform fault in Tierra del Fuego. EOS Trans. AGU 83 (1), 1+5–6.

Lodolo, E., Menichetti, M., Bartole, R., Ben-Avraham, Z., Tassone, A., Lippai, H., 2003. Magallanes-Fagnano continental transform fault (Tierra del Fuego, southernmost South America). Tectonics 22 (6), 1–26.

Lodolo, E., Lippai, H., Tassone, A., Zanolla, C., Menichetti, M., Hormaechea, J.L., 2007. Gravity map of the Isla Grande de Tierra del Fuego, and morphology of Lago Fagnano. Geol. Acta 4, 307–314.

Lodolo, E., Baradello, L., Darbo, A., Caffau, M., Tassone, A., Lippai, H., Lodolo, A., De Zorzi, G., Grossi, M., 2012. Occurrence of shallow gas in the easternmost Lago Fagnano (Tierra del Fuego). Near Surf. Geophys. Nr. 10, 161–169.

Lodolo, E., Lozano, J., Donda, F., Bran, D., Baradello, L., Tassone, A., Romeo, R., Paterlini, M., Grossi, M., Caffau, M., Vilas, J.F., 2020a. Late-glacial fluctuations of two southern Patagonia outlet glaciers revealed by high-resolution seismic surveys. Quat. Res. 97, 111–124. https://doi.org/10.1017/qua.2020.20.

Lodolo, E., Donda, F., Lozano, J., Baradello, L., Romeo, R., Bran, D.M., Tassone, A., 2020b. The submerged footprint of Perito Moreno glacier. Sci. Rep. 10 (16437), 1–10. https://doi.org/10.1038/s41598-020-73410-8.

Lozano, J.G., Donda, F., Bran, D., Lodolo, E., Baradello, L., Romeo, R., Vilas, J.F., Grossi, M., Tassone, A., 2020. Depositional setting of the southern arms of Lago Argentino (southern Patagonia). J. Maps 16 (2), 324–334. https://doi.org/10.1080/17445647.2020.1746700.

Lozano, J.G., Tassone, A., Lodolo, E., Menichetti, M., Cerredo, M.E., Bran, D.M., Esteban, F., Ormazabal, J.P., Baradello, L., Vilas, J.F., 2018a. Geophysical survey in Lago Yehuin, Isla Grande de Tierra del Fuego, Argentina: origin and evolution. Andean Geol. 45 (3), 318–343. https://doi.org/10.5027/andgeoV45n3-3085.

Lozano, J.G., Tassone, A., Bran, D.M., Lodolo, E., Menichetti, M., Cerredo, M.E., Esteban, F., Ormazabal, J.P., Ísola, J., Baradello, L., Vilas, J.F., 2018b. Glacial-related morphology and sedimentary setting of a high-latitude lacustrine basin: The Lago Chepelmut (Tierra del Fuego, Argentina). J. S. Am. Earth Sci. 86, 259–270. https://doi.org/10.1016/j.jsames.2018.06.020.

Lozano, J.G., Bran, D.M., Donda, F., Lodolo, E., Esteban, F.D., Tassone, A., 2021a. Palaeolago fueguino. a Late Pleistocene lacustrine basin located in the central sector of Tierra del Fuego: A seismostratigraphic study. Journal of Quaternary Science 36 (2), 273–287. https://doi.org/10.1002/jqs.3276.

Lozano, J.G., Bran, D.M., Lodolo, E., Tassone, A., Vilas, J.F., 2021b. Holocene seismic stratigraphy of the southern arms of Lago Argentino. J. S. Am. Earth Sci. 111, 103495 https://doi.org/10.1016/j.jsames.2021.103495.

Lozano, J.G., Gutierrez, Y., Bran, D.M., Lodolo, E., Cerredo, M.E., Tassone, A., Vilas, J.F., 2022. Structure, seismostratigraphy and tectonic evolution of Lago Roca (southern Patagonia, Argentina). Geol. J. 57 (8), 3101–3113. https://doi.org/10.1002/gj.4454.

Malz, P., Meier, W., Casassa, G., Jaña, R., Skvarca, P., Braun, M., 2018. Elevation and mass changes of the southern Patagonia icefield derived from TanDEM-X and SRTM data. Rem. Sens. 10, 188.

Malagnino, E.C., Strelin, J.A., 1990. Variations of Upsala Glacier in Southern Patagonia since the Late Holocene to the Present. Glaciological researches in Patagonia, pp. 61–85.

McCulloch, R.D., Bentley, M.J., 1998. Late glacial ice advances in the Strait of Magellan, southern Chile. Quat. Sci. Rev. 17, 775–787.

McCulloch, R.D., Bentley, M.J., Purves, R.S., Hulton, N.R.J., Sugden, D.E., Clapperton, C. M., 2000. Climatic inferences from glacial and palaeoecological evidence at the last glacial termination, southern South America. J. Quat. Sci. 15, 409–417.

Mercer, J.H., 1969. Glaciation in Southern Argentina. More than two million years ago. Science 164 (3881), 823–825.

Mercer, J.H., 1976. Glacial history of southernmost South America. Quat. Res. 6, 125–166.

Minowa, M., Sugiyama, S., Sakakibara, D., Skvarca, P., 2017. Seasonal variations in icefront position controlled by frontal ablation at glaciar Perito Moreno, the southern Patagonia icefield. Front. Earth Sci. 5, 1. https://doi.org/10.3389/feart.2017.00001.

Nullo, F.E., Blasco, G., Risso, C., Combina, A., Otamendi, J., 2006. Hoja Geológica 5172-I y 5175-II El Calafate, provincia de Santa Cruz. Instituto de Geología y Recursos Minerales. Servicio Geológico Minero Argentino.

Patton, H., Swift, D.A., Clark, C.D., Livingstone, S.J., Cook, S.J., 2016. Distribution and characteristics of overdeepenings beneath the Greenland and Antarctic ice sheets: implications for overdeepening origin and evolution. Quat. Sci. Rev. 148, 128–145.

Preusser, F., Reitner, J.M., Schluechter, C., 2010. Distribution, geometry, age and origin of overdeepened valleys and basins in the Alps and their foreland. Swiss J. Geosci. 103, 407–426.

Quirós, R., Baigún, C.R.M., Cuch, S., Delfino, R., De Nichilo, A., Guerrero, C., Marinone, M.C., Menu Marque, S., Scapini, M.C., 1988. Evaluación del Rendimiento Pesquero Potencial de la República Argentina: I. Datos 1. Informe Técnico N° 7 del Departamento de Aguas Continentales. Instituto Nacional de Investigación y Desarrollo Pesquero (INIDEP), p. 55.

Sakakibara, D., Sugiyama, S., 2014. Ice-front variations and speed changes of calving glaciers in the Southern Patagonia Icefield from 1984 to 2011. J. Geophys. Res. Earth Surf. 119, 2541–2554. https://doi.org/10.1002/2014JF003148.

Skvarca, P., Naruse, R., 2006. Overview of the ice-dam formation and collapse of glaciar Perito Moreno, southern Patagonia, in 2003/04. J. Glaciol. 52 (178), 476–478.

Skvarca, P., De Angelis, H., Naruse, R., Warren, C.R., Aniya, M., 2002. Calving rates in fresh water: new data from southern Patagonia. Ann. Glaciol. 34, 379–384.

Strelin, J.A., Malagnino, E.C., 2000. Late-glacial history of Lago Argentino, Argentina, and age of the Puerto Bandera moraines. Quat. Res. 54, 339–347.

Strelin, J.A., Malagnino, E.C., 1996. GLACIACIONES PLEISTOCENAS del lago argentino Y alto valle del río santa cruz. Congreso Geológico Argentino y III Congreso de Exploración de Hidrocarburos, Actas IV, 311–325.

Strelin, J., Denton, G., Vandergoes, M., Ninnemann, U., Putnam, A., 2011. Radiocarbon chronology of the late-glacial Puerto Bandera moraines, southern patagonian icefield, Argentina. Quat. Sci. Rev. 30, 2551–2569.

Strelin, J.A., Kaplan, M.R., Vandergoes, M.J., Denton, G.H., Schaefer, J.M., 2014. Holocene glacier history of the Lago Argentino basin, southern patagonian icefield. Quat. Sci. Rev. 101, 124–145.

Stuefer, M., Rott, H., Skvarca, P., 2007. Glaciar Perito Moreno, Patagonia: climate sensitivities and glacier characteristics preceding the 2003/04 and 2005/06 damming events. J. Glaciol. 53, 3–16.

Swift, D.A., Persano, C., Stuart, F.M., Gallagher, K., Whitham, A., 2008. A reassessment of the role of ice sheet glaciation in the long-term evolution of the East Greenland fjord region. Geomorphology 97, 109–125.

Thorndycraft, V.R., Bendle, J.M., Benito, G., Davies, B.J., Sancho, C., Palmer, A.P., Fabel, D., Medialdea, A., Martin, J.R.V., 2019. Glacial lake evolution and Atlantic-Pacific drainage reversals during deglaciation of the Patagonian Ice sheet. Quaternary Sience Reviews 203, 102–127.

Van Wyk de Vries, M., Ito, E., Shapley, M., Brignone, G., Romero, M., Wickert, A.D., Miller, L.H., MacGregor, K.R., 2022. Physical limnology and sediment dynamics of Lago Argentino, the world's largest ice-contact lake. J. Geophys. Res.: Earth Surf. 127 (3), e2022JF006598.

Waldmann, N., Ariztegui, D., Anselmetti, F.S., Austin, Jr.J.A., Dunbar, R.B., Moy, C.M., Recasens, C., 2008. Seismic stratigraphy of Lago Fagnano sediments (Tierra del Fuego, Argentina) - a potential archive of Paleoclimatic change and tectonic activity since the Late Glacial. Geol. Acta 6, 101–110.

Waldmann, N., Ariztegui, D., Anselmetti, F.S., Austin, Jr.J.A., Moy, C.M., Stern, C., Recasens, C., Dunbar, R.B., 2009. Holocene climatic fluctuations and positioning of the Southern Hemisphere westerlies in Tierra del Fuego (54°S), Patagonia. J. Quat. Sci. 25 (7), 1063–1073.

Waldmann, N., Ariztegui, D., Anselmetti, F.S., Coronato, A., Austin, Jr.J.A., 2010a. Geophysical evidence of multiple glacier advances in Lago Fagnano (54°S), southernmost Patagonia. Quat. Sci. Rev. 29, 1188–1200.

Waldmann, N., Anselmetti, F.S., Ariztegui, D., Austin Jr, J.A., Pirouz, M., Moy, C.M., Dunbar, R., 2010b. Holocene mass-wasting events in Lago Fagnano, Tierra del Fuego (54° S): implications for paleoseismicity of the Magallanes-Fagnano transform fault. Basin Res. 23 (2), 171–190.

Zamorano Morales, D.A., 2020. Influencia geológica en la dinámica de los glaciares O'Higgins. Viedma y Upsala en campo de hielo Patagónico Sur. Universidad de Chile -. Facultad de Ciencias Físicas y Matemáticas, Santiago, Chile. https://repositorio.uchile.cl/handle/2250/178290.

Zanolla, C., Lodolo, E., Lippai, H., Tassone, A., Menichetti, M., Baradello, L., Grossi, M., Hormaechea, J.L., 2011. Bathymetric map of Lago Fagnano (Tierra del Fuego Island). Boll. Geofis. Teor. Appl. 52, 1–8.